

This article was downloaded by:

On: 25 January 2011

Access details: *Access Details: Free Access*

Publisher *Taylor & Francis*

Informa Ltd Registered in England and Wales Registered Number: 1072954 Registered office: Mortimer House, 37-41 Mortimer Street, London W1T 3JH, UK



## Separation Science and Technology

Publication details, including instructions for authors and subscription information:

<http://www.informaworld.com/smpp/title~content=t713708471>

### Spherical Resorcinol-Formaldehyde Resin Testing for Cesium Removal from Hanford Tank Waste Simulant

S. K. Fiskum<sup>a</sup>; D. L. Blanchard<sup>a</sup>; M. J. Steele<sup>a</sup>; K. K. Thomas<sup>a</sup>; T. Trang-Le<sup>a</sup>; M. R. Thorson<sup>b</sup>  
<sup>a</sup> Battelle—Pacific Northwest Division, Richland, WA, USA <sup>b</sup> Washington Group International, Richland, WA, USA

**To cite this Article** Fiskum, S. K. , Blanchard, D. L. , Steele, M. J. , Thomas, K. K. , Trang-Le, T. and Thorson, M. R.(2006) 'Spherical Resorcinol-Formaldehyde Resin Testing for Cesium Removal from Hanford Tank Waste Simulant', *Separation Science and Technology*, 41: 11, 2461 – 2474

**To link to this Article:** DOI: 10.1080/01496390600742740

URL: <http://dx.doi.org/10.1080/01496390600742740>

## PLEASE SCROLL DOWN FOR ARTICLE

Full terms and conditions of use: <http://www.informaworld.com/terms-and-conditions-of-access.pdf>

This article may be used for research, teaching and private study purposes. Any substantial or systematic reproduction, re-distribution, re-selling, loan or sub-licensing, systematic supply or distribution in any form to anyone is expressly forbidden.

The publisher does not give any warranty express or implied or make any representation that the contents will be complete or accurate or up to date. The accuracy of any instructions, formulae and drug doses should be independently verified with primary sources. The publisher shall not be liable for any loss, actions, claims, proceedings, demand or costs or damages whatsoever or howsoever caused arising directly or indirectly in connection with or arising out of the use of this material.

## Spherical Resorcinol-Formaldehyde Resin Testing for Cesium Removal from Hanford Tank Waste Simulant

**S. K. Fiskum, D. L. Blanchard, M. J. Steele, K. K. Thomas,  
and T. Trang-Le**

Battelle—Pacific Northwest Division, Richland, WA, USA

**M. R. Thorson**

Washington Group International, Richland, WA, USA

**Abstract:** A new spherical form of resorcinol-formaldehyde (RF) resin was tested for efficacy of cesium removal from Hanford tank waste. Two spherical RF formulations, prepared by varying curing temperature, were tested. Both resins had a tight particle size distribution and a high degree of sphericity. Small-scale column testing (on ~20-mL resin beds) was conducted evaluating the cesium load profile with AZ-102 simulated tank waste and the cesium elution profile using 0.5 M HNO<sub>3</sub> eluant. The load and elution profiles were compared in side-by-side testing with ground-gel RF resin and SuperLig® 644, the Waste Treatment Plant baseline ion exchanger. Although breakthrough capacity was not as high as the other resins tested, the spherical RF resin met plant cesium loading requirements with the AZ-102 simulant matrix. Excellent reproducibility of cesium load and elution was demonstrated over three process cycles with no evidence of degraded performance. Residual cesium on the resin beds after elution was nearly a factor of 10 lower than that of the ground-gel RF and SuperLig® 644.

**Keywords:** Resorcinol-formaldehyde resin, SuperLig® 644, cesium ion exchange, Hanford tank waste

### INTRODUCTION

Liquid wastes, generated during 40 years of plutonium production at the Hanford Site near Richland, Washington, are estimated to contain 40 MCi

Received 20 October 2005, Accepted 22 March 2006

Address correspondence to S. K. Fiskum, Battelle—Pacific Northwest Division, P7-22, P.O. Box 999, Richland, WA 99352, USA. E-mail: sandyfiskum@pnl.gov

<sup>137</sup>Cs fission product distributed across a volume of 55-million gallons (1). The liquid wastes are complex mixtures containing high concentrations of sodium nitrate, nitrite, and hydroxide, as well as a myriad of minor and trace inorganic, organic, and radioisotopic constituents. The wastes are intended to be vitrified into monolithic glass at the River Protection Project-Waste Treatment Plant (RPP-WTP) in preparation for long-term geologic disposal. The RPP-WTP requires most of the <sup>137</sup>Cs to be removed from the bulk of the liquid such that two different vitrified waste products can be produced:

1. low-activity waste with minimal <sup>137</sup>Cs loading containing the bulk of the dissolved salt constituents (high volume fraction), and
2. high-activity waste containing the bulk of the <sup>137</sup>Cs along with the <sup>90</sup>Sr and transuranic components (low volume fraction).

The baseline pretreatment technology for cesium removal requires processing on an elutable and reusable ion exchanger.

Parameters for selecting ion exchange material include physical stability, chemical stability, regeneration efficiency, low leakage, high selectivity, and high capacity, as well as ability to sustain high flowrates with low pressure drops (2). Large particles with a narrow size distribution are optimal for the latter parameters. A small particle size favors rapid kinetic exchange and low leakage as it is directly proportional to surface area (influencing film diffusion). Optimization of hydraulic properties is generally balanced with optimizing exchange kinetics.

The organic ground-gel ion exchanger SuperLig®-644 is currently the baseline resin for the RPP-WTP. It has demonstrated high cesium capacity and selectivity from representative tank wastes, including high-organic wastes, high-potassium wastes, and high-sulfate wastes (3). However, SuperLig®-644 has presented the RPP-WTP with several challenges. It is only available through a sole-source, IBC Advanced Technology (American Fork, Utah); its formulation is proprietary; it is expensive; and its physical properties tend to result in hydraulic processing issues.

Resorcinol-formaldehyde (RF) was selected as the most promising alternative to SuperLig®-644. Ground-gel RF resin (Boulder Scientific Corporation, Colorado) had been previously studied for use with Hanford tank wastes (4–7). However, the ground-gel RF resin shares the undesirable morphological characteristic with SuperLig®-644 deriving from the fact that both are granular materials with intrinsic irregular shape and large particle size distribution (PSD) along with significant shrink-swell effects.

A formulation patent for loading RF into an engineered mono-disperse bead was found. The bead morphology lends distinct advantages to column processing with regard to resin packing and fluid flow. The new RF resin formulation required physical property and performance testing in side-by-side comparisons with SuperLig®-644 and ground-gel RF in an effort to

evaluate its efficacy for use in the RPP-WTP. Surface and cross-section morphology was evaluated as well as resin density and PSD. Column process testing was conducted to evaluate cesium breakthrough capacity, selectivity, shrink/swell characteristics, elutability and regenerability using Hanford AZ-102 tank waste simulant.

## EXPERIMENTAL

Two spherical RF resins, one cured at a low temperature (#3) and the other cured at a higher temperature (#4), were obtained from the patent-holder. Two SuperLig®-644 resin lots were tested: lot number C-01-05-28-02-35-60 (35- to 60-mesh) and C-01-11-05-02-35-60 (wet sieved at Savannah River National Laboratory to 18- to 40-mesh (8)), each in the sodium-form. The potassium-form ground-gel RF, lot number BSC-187-1-0002, was obtained from Boulder Scientific Corporation (Mead, CO).

Each resin was pretreated before testing by cycling between the hydrogen-form and sodium-form. Each resin (as-received) was converted to the hydrogen-form by contacting it with 0.5 M HNO<sub>3</sub> in a 3 to 1 ratio of liquid-to-resin volume for 1 hour with occasional gentle swirling. The acid was decanted, and the resin was rinsed with deionized (DI) water in a 3-to-1 ratio of liquid-to-resin volume for 10 minutes with gentle swirling. The DI water rinse was repeated until the contact solution pH was >4 or a minimum of three times. The resin was then contacted with 0.25 M NaOH in a 3-to-1 ratio of liquid-to-resin volume for 2 hours with occasional gentle swirling. The basic solution was then decanted, and the resin was rinsed with DI water as previously described. This DI water rinse was repeated until the solution pH was <10 for a minimum of three times. The acid-base conversion was then repeated once. All resins were converted back to hydrogen-form by repeating the acid contact and DI water rinse.

The pretreated resins were dried under flowing nitrogen and/or under vacuum (25 mm Hg) at ambient temperature until they were free-flowing and had a nearly constant mass. The resins still contained some moisture but could be representatively sub-sampled. Weighed aliquots were then split for various testing activities. At the same time, duplicate aliquots were split to determine total moisture content. Moisture content was determined from mass difference after drying under vacuum at 50°C to constant mass. The hydrogen-form resin masses loaded in the ion exchange columns were corrected for moisture content. All resin mass measures were based on the dry hydrogen-form.

Optical micrographs of the pretreated resins were taken at 70 $\times$  magnification to characterize particle shape and morphology. Several observations were made of the resin before the micrographs were taken to help ensure that the photographed regions were representative of the overall resin. The PSD was measured on each of the pretreated resins in both the hydrogen-form and the sodium-form using a Micro TRAC S3000 Particle Size

Analyzer. The dispersion liquid for both the hydrogen-form and the sodium-form resins was DI water.

Before ion exchange testing, an aliquot of the pre-treated hydrogen-form resin was soaked in a 10:1 solution-to-resin volume ratio of 1 M NaOH. After 2 hours, the NaOH was decanted, water was added, and the resin slurry was transferred to the column. The resin bed was rinsed with DI water and cycled to the hydrogen-form with 0.5 M HNO<sub>3</sub> and back to the sodium-form with 0.5 M NaOH. The swollen sodium-form resin bed volumes were nominally 20 mL, 6 cm tall and 2 cm diameter with length to diameter ratio of 3. The fluid level above the resin bed was maintained at nominally the 9.5-mL height relative to the bottom of the resin bed. Depending on whether the resin was expanded (nominally 6 cm tall in the sodium-form) or contracted (nominally 4 cm tall in the hydrogen-form), fluid volume above the resin bed varied from nominally 9 mL to 17 mL, consistent with the plant operating conditions.

The ion exchange column assembly is shown in Fig. 1. Custom made ion exchange columns (Kontes Custom Glass Shop, Vineland, NJ) were 10-cm tall with an inside diameter of 2.0 cm (corresponding to a resin volume of 3.1 mL/cm). The resin beds were supported on stainless steel, 200-mesh screens. The end fittings were standard Kontes Chromaflex® column end fittings with Teflon ferrules connected to 1/16-in. ID Teflon™ tubing. The column assembly contained an in-line Swagelok Poppet pressure relief check valve with a 10-psi trigger (Solon, OH) and a 15-psi pressure gauge (McDaniel

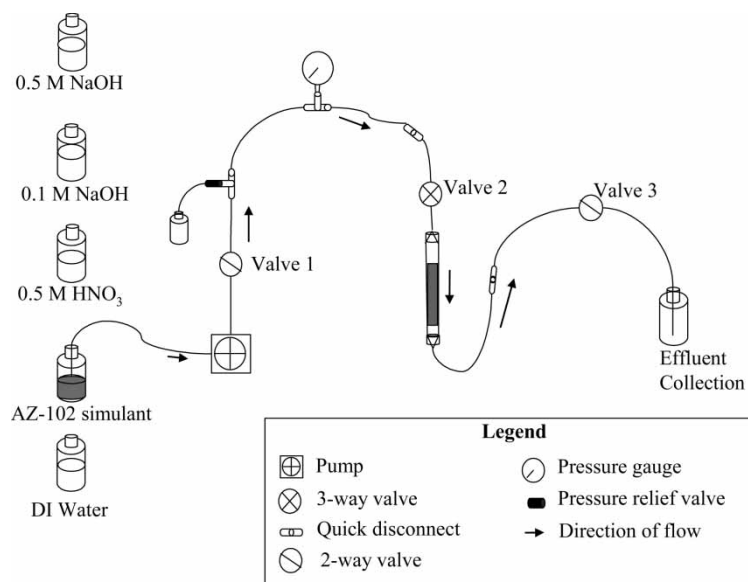


**Figure 1.** Schematic of the ion exchange test apparatus.

Controls Model #SA, Luling, LA). Valved quick-disconnects (Cole Parmer, Vernon Hills, IL) were installed in-line to allow for ease of column removal. Fluid Metering, Incorporated (FMI) QVG50 pumps (Syosset, NY) equipped with a ceramic and Kynar® coated low-flow piston pump heads were used to introduce all fluids. The flowrate was controlled with a remotely operated FMI stroke-rate controller. The holdup volume of the entire ion exchange system was nominally 50 mL, the summed volume of all fluid-filled parts.

All processing was conducted downflow. Load and elute conditions were established to mimic process plant operations. Table 1 shows the nominal process conditions. The fourth process cycle feed was introduced at a very slow flow rate of 0.73 BV/h.

The AZ-102 simulant, containing 50 µg/mL Cs, was prepared by Noah Technologies (San Antonio, Texas) as previously described (9). Table 2 provides the simulant composition. Just before processing, solids were removed by filtering through a 0.5-µm pore size nylon filter. The simulant feed was spiked with radioactive cesium tracer. Initial tests were conducted with 0.013 mCi/L  $^{134}\text{Cs}$  tracer; later tests were conducted at higher tracer concentration, 0.075 mCi/L  $^{137}\text{Cs}$ , to improve evaluation of high decontamination factors. Effluent samples were collected periodically during simulant feed and elution steps to measure cesium breakthrough and elution behavior. The cesium tracer was measured using gamma spectrometry. Detection limits for both isotopes were nominally 7E-7 mCi/L (14-h count time). Count times were adjusted for samples greater than the detection limit to minimize uncertainty (typically  $\pm 5\%$ ). After a process cycle was completed, the ion exchange column assembly was disconnected at the quick disconnects and removed for direct gamma energy analysis of residual cesium tracer on the resin bed.

The resin bed densities were determined during column processing and were based on the observed resin bed height, calculated volume, and dry

**Table 1.** Nominal process conditions

Step	Feed	Flowrate (BV/h)	Volume (BV)
Load	AZ-102 Simulant	1.5 <sup>a</sup>	120 to 250 <sup>c</sup>
Displace	0.1 M NaOH	3	3.5
Rinse	Water	3	3.5
Elute	0.5 M HNO <sub>3</sub>	2/1.4 <sup>b</sup>	6/20–30 <sup>b</sup>
Rinse	Water	1.4	3
Regenerate	1.0 M NaOH (RF) 0.25 NaOH (SuperLig®-644)	3	6

<sup>a</sup>The fourth process cycle feed flowrate was 0.73 BV/h.

<sup>b</sup>The elution started at 2 BV/h for the first six BV, and then the flow rate was reduced to 1.4 BV/h.

<sup>c</sup>Process volume depended on resin performance.

**Table 2.** AZ-102 simulant composition

Analyte	Average $\mu\text{g/mL}^a$	Average $\text{M}^a$
Cs	48.7	3.66E-4
Al	1,360	5.04E-2
Cr	1,450	2.79E-2
K	5,720	1.46E-1
Na	119,500	5.20E + 0
P	323	1.04E-2
$\text{Cl}^-$	40	1.13E-3
$\text{NO}_2^-$	54,600	1.19E + 0
$\text{NO}_3^-$	30,400	4.90E-1
$\text{PO}_4^{3-}$	945	9.95E-3
$\text{SO}_4^{2-}$	30,000	3.12E-1
$\text{OH}^-$	3,540	2.08E-1
C (as carbonate)	10,900	9.08E-1
C (as organic carbon)	11,200	9.33E-1
Density	1.233 g/mL at 23°C	

<sup>a</sup>The overall uncertainty is  $\pm 15\%$ .

hydrogen-form resin mass. Shrink swell characteristics were determined from resin bed height measures during in-column testing.

## RESULTS AND DISCUSSION

### Physical Properties

The morphologies of spherical RF, ground-gel RF, and SuperLig®-644 are presented in Fig. 2. The ground-gel RF and SuperLig®-644 appeared nearly identical with irregular sized pieces with smooth faces and angular edges. In contrast, the spherical RF resins were uniformly sized, relatively smooth, and uniformly spherical. Figure 3 provides scanning electron micrographs of the surface and cross section of spherical RF #3. A distinct core was evident that may represent incompletely reacted or cured product. The RF #4 (not shown) had a similar appearance.

The ground gels resulted in broad PSDs; the spherical RF resin PSDs were virtually mono-disperse. The sodium-form PSD averages and low 10% to high 90% ranges, on a volume distribution basis, are shown in Fig. 4. The hydrogen-form particle size spreads were similar except particle diameters of the spherical resins were about 15% smaller. The broad particle size ranges of the ground-gel resins are typical and consistent with the manufacturing process (condensation polymerization) where the reacted product is mechanically ground to the desired mesh size. The tight PSD of the spherical resins was specifically controlled via the patented production process.

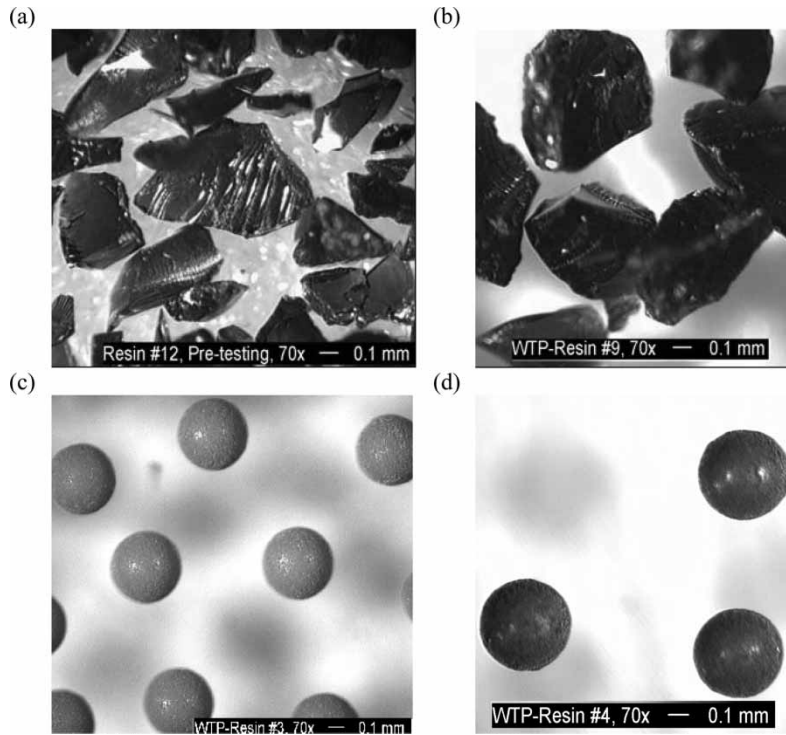


**Figure 2.** Resin micrographs, (a) SuperLig®-644 (35- to 60-mesh), (b) ground-gel RF, (c) spherical RF Resin #3, (d) spherical RF Resin #4.

All resins expanded on conversion from hydrogen-form to sodium-form. Both SuperLig®-644 test resins expanded the most at 58% (35- to 60-mesh) and 43% (18- to 40-mesh) on conversion from hydrogen to sodium form; the ground-gel RF resin expanded 33%, and both spherical RF resins

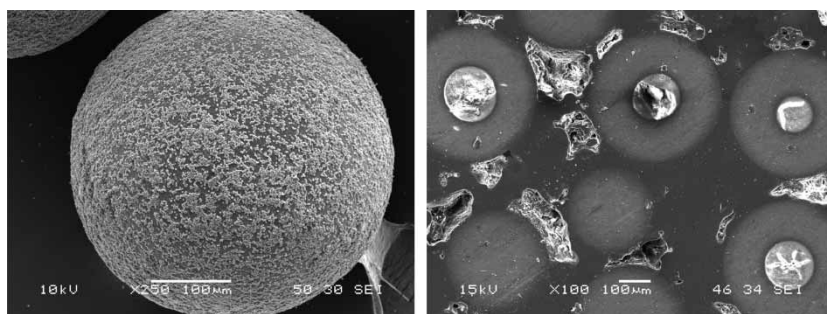


**Figure 3.** SEM micrographs of spherical RF Resin #3, surface and cross-sections (embedded in epoxy).

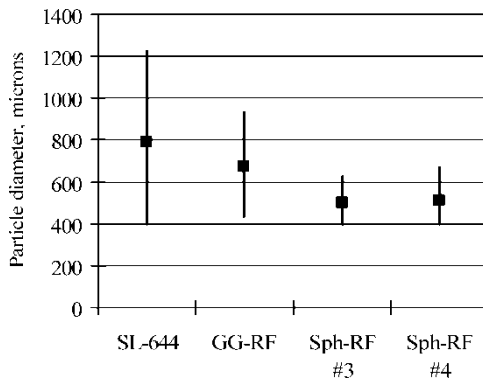


**Figure 4.** Particle size distribution of sodium-form resins, showing mean and 10% to 90% range (volume basis).

expanded the least at 30%. The resins similarly contracted when returned to the hydrogen-form (elution condition). Resin fines have been observed in effluents during repeated cycling of SuperLig®-644 (10). The fines were conjectured to result from fracturing during the expansion and contraction processes. Only particles small enough for entrainment would appear in the effluent solution; larger broken pieces would remain in the interstitial spaces in the resin bed. Filling the interstices would lead to large pressure drops across the resin bed. The spherical resin shape has no specifically vulnerable areas of fracture during expansion and contraction. Repeated processing (3.5 cycles) with the spherical resins resulted in no discernable fines production.

### Cesium Loading

The cesium load profiles for the three resin types are shown in Fig. 5. The cesium effluent concentration ( $C$ ) is shown as a ratio to the feed cesium concentration ( $C_o$ ) on a probability scale (y-axis). The number of bed volumes processed (volume of resin in the sodium-form regeneration condition) is provided on a linear scale (x-axis). Load performance comparisons were evaluated from three perspectives: bed volumes (BVs) processed to the onset of breakthrough, BVs processed to 50% breakthrough (breakthrough capacity), and linearity of load curve on the probability plot. Evaluation of the onset of breakthrough was limited by the effluent cesium tracer detection capability. In the case of the spherical RF and the 18- to 40-mesh SuperLig®-644, higher tracer concentrations were used, enabling lower  $C/C_o$  detection limits. Because all resins displayed ideal load characteristics (based on the linear breakthrough profile on the probability plot), comparisons of breakthrough onset were approximated by extrapolating the breakthrough

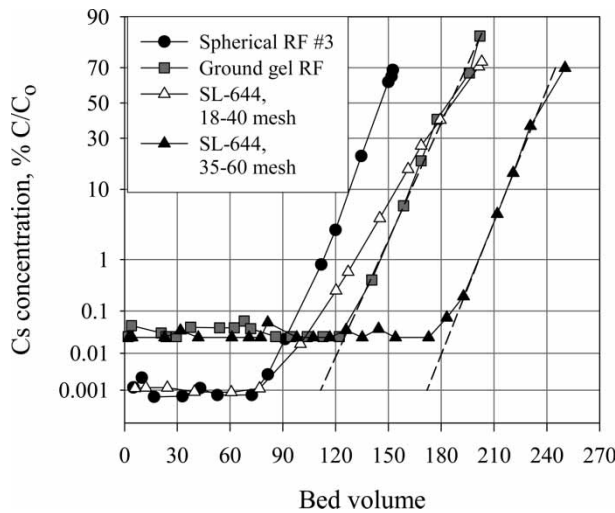


**Figure 5.** Breakthrough profiles with AZ-102 simulant, 49 mg/L Cs, 1.5 BV/h flowrate showing extrapolation to 0.001% C/C<sub>0</sub>.

curves for ground-gel RF and 35- to 60-mesh SuperLig® 644 down to 0.001% C/C<sub>0</sub> detection limit.

The two baseline SuperLig®-644 test resins resulted in substantially different load profiles. The smaller PSD (35- to 60-mesh) material cesium breakthrough (onset and 50%) was nominally 60 BVs greater than that of the larger particle size (18- to 40-mesh) fraction. Production parameters of the larger PSD material may have been altered slightly to reduce the shrink-swell change at the expense of cesium capacity. The spherical RF #3 resin resulted in 0.001% cesium breakthrough after processing nominally 78 BV, similar to the large PSD SuperLig®-644. The ground-gel RF onset of breakthrough was between the two different SuperLig®-644 test resins: its breakthrough capacity was similar to that of the 18- to 40-mesh SuperLig®-644. The spherical RF resins had the lowest capacity; the RF #3 50% cesium breakthrough was 145 BVs.

Figure 6 demonstrates the reproducibility of the spherical RF resins cesium load profiles. Over the 3.5 load cycles tested, there was no measurable difference in the breakthrough profiles. Within the experimental parameters, there was no evidence of cesium bleed or cross-contamination from one process cycle to the next. The higher cure temperature of spherical RF#4 clearly had a significant impact on the cesium capacity, reducing the cesium 50% breakthrough from 145 BVs (#3) to 85 BVs. The fourth process cycle, conducted at half the flowrate, showed an improved performance where breakthrough was not observed up to 60 BVs, indicating that cesium exchange may be particle diffusion-limited. Other permutations in production parameters

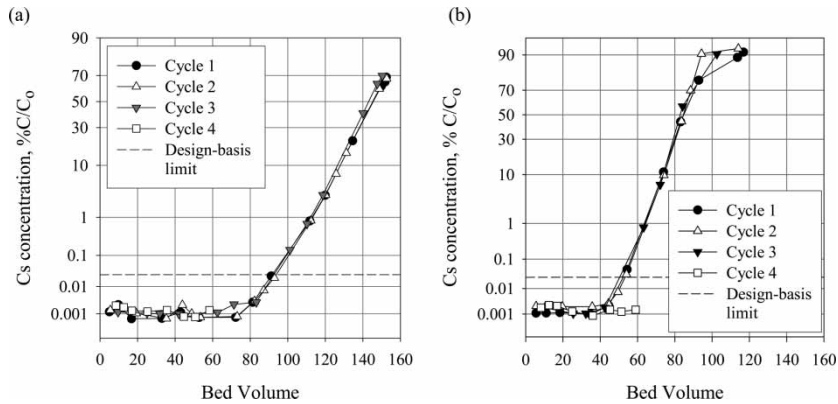


**Figure 6.** Breakthrough profiles for spherical RF Resin #3 (a) and #4 (b), 3.5 process cycles, AZ-102 simulant, 49 mg/L Cs, 1.5 BV/h flowrate.

may be applicable to enhance the load performance relative to RF #3. Despite its decreased performance, RF #4 still would have satisfied the plant performance criterion. Only 25 BV of the high-cesium AZ-102 type feed is expected to be processed in one cycle in order to limit the total  $^{137}\text{Cs}$  Curie loading in the column. The single-column effluent cesium concentration remained below the bulk cesium breakthrough contract limit of 0.025%  $\text{C}/\text{C}_0$  (the contract limit applies to effluent from three serial columns). Larger volumes of other tank wastes will be processed in each process cycle at the RPP-WTP.

Table 3 provides the calculated cesium loading at 50% breakthrough under the given process condition for the AZ-102 simulant matrix. The breakthrough capacities are provided in two contexts: a dry hydrogen-form resin mass basis and an expanded sodium-form resin volume basis. SuperLig®-644 clearly had the higher (47 mg/g) breakthrough capacity on a per gram basis. The spherical RF #4 with the higher temperature cure had the least breakthrough capacity (14 mg/g). On a mass basis, the breakthrough capacity of the spherical RF #3 was nearly equivalent to that of the ground-gel RF. When compared on an expanded resin volume basis, the resin breakthrough capacity differences significantly narrowed. Additional testing is ongoing to optimize the spherical RF formulation to improve capacity. In part, this may be effected by filling in the apparent “hollow” core (shown in Fig. 3).

### Elutability

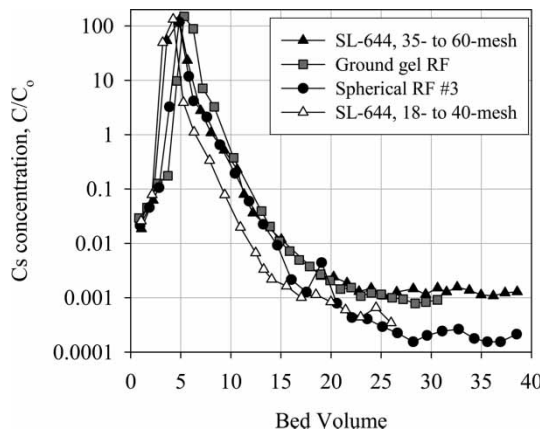
Cesium was quickly and efficiently eluted from all resin types with 0.5 M nitric acid. Figure 7 provides elution profile comparisons. The peak cesium concentration was found during the fifth BV collection. Cesium effluent concentration quickly tapered to a constant  $\text{C}/\text{C}_0$  after processing 26 bed volumes

**Table 3.** Relative resin bed densities and cesium loading at 50%  $C/C_o$ 

	Bed density, g H-form resin per mL expanded Na-form resin	mg Cs/g dry H-form resin	mg Cs/mL expanded Na-form resin
SuperLig®-644 (35- to 60-mesh)	0.21	47	12
SuperLig®-644 (18- to 40-mesh)	0.21	40	9
Ground gel RF	0.36	25	8
Spherical RF #3	0.25	22	6
Spherical RF #4	0.25	14	3

for all resins. The significant difference in the elution characteristics between the resins was manifested at the tail region where the spherical RF reached nearly a factor of five less residual cesium effluent concentration than those of the ground-gel RF and SuperLig®-644 (35- to 40-mesh). The trend for SuperLig®-644 (18- to 40-mesh) was not followed sufficiently long to evaluate the relative cesium eluate concentration through the tail. The final eluate samples taken indicated that the residual cesium effluent concentration may have been comparable to that achieved by the spherical RF.

The post-elution relative mass of residual cesium on a per gram dry hydrogen-form resin basis is shown in Fig. 8. Residual cesium on the post-eluted spherical RF resin bed was consistently less, by nearly an order of magnitude, than those of the ground-gel RF and SuperLig®-644. Both SuperLig®-644 test resins resulted in similar residual cesium loading at 2.7  $\mu\text{g}$  (35- to 60-mesh) and 3.5  $\mu\text{g}$  (18- to 40-mesh) cesium per g dry

**Figure 7.** Elution profiles for four test resins, 0.5 M  $\text{HNO}_3$  eluant at 2 BV/h (1–6 BV) then 1.4 BV/h.

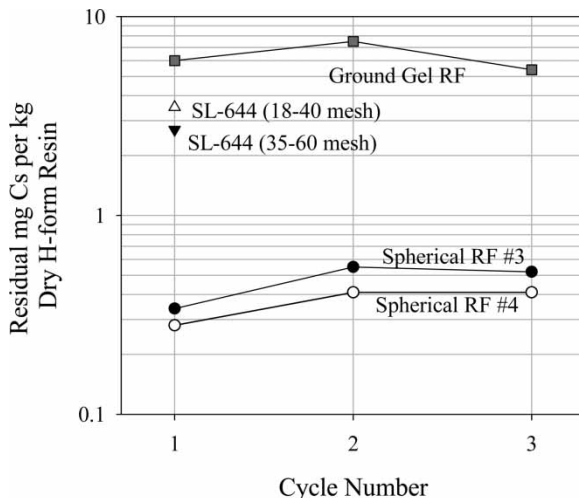


Figure 8. Residual cesium on resin beds, post elution.

hydrogen-form resin, despite the 20% difference in peak cesium mass loadings, 47 mg/g and 40 mg/g, respectively. The higher cesium concentration still bound to the large PSD SuperLig®-644 resin may be attributed to the shorter elution volume (26 BV vs 36 BV) of the test and/or limitations of cesium particle diffusion in the contracted resin particles. The observed residual cesium resin concentrations were consistent with previously-reported quantities of 1.7 µg/g (11) and 2.9 µg/g (12). The residual cesium in ground-gel RF ranged from 5 to 8 µg/g dry hydrogen-form resin (following a nominal loading of 25 mg Cs/g). The spherical RF held only 0.28 to 0.55 µg cesium per g dry hydrogen-form resin. Resin #3 was loaded to a similar extent as the ground-gel RF; Resin #4 had nominally half the cesium mass loading.

The post-elution residual cesium on the resin bed has significance for follow-on processing. The more cesium on the resin, the more cesium contamination from bleed is expected in the next process cycle effluent and the lower the achievable decontamination factor. Residual cesium in spent resin will contribute to the dose rate of the waste form in proportion to the isotopic fraction of  $^{137}\text{Cs}$ . As the cesium concentration increases, the more waste containment shielding, and thus cost, of the spent resin will be required for disposal.

### Plant Processing Considerations

The RF resin resulted in less cesium loading than the baseline SuperLig®-644 material with the AZ-102 simulant. This may be a result of less capacity

and/or less selectivity. The lower capacity/selectivity is not necessarily problematical for plant operations. Threshold concentrations of  $^{137}\text{Cs}$  have been set based on maximum dose allowed for the resin material, in-column heat generation, and general area dose rate in the plant. The current process flow sheet loads nominally 25 BVs of the AZ-102 tank waste to meet the production rate criterion. This limit is less than half of the 50% breakthrough obtained on the poorer performing spherical RF #4 resin. Current test activities are evaluating modified spherical RF formulations and curing parameters to improve capacity.

The AZ-102 simulant is a low-potassium waste, typical of the bulk of the waste feeds that will be processed at the WTP. Potassium is a strong competitor for cesium on these ion exchange resins. SuperLig<sup>®</sup>-644 has been formulated to work well in a high-potassium waste. It is anticipated that the RF resin will be less tolerant of potassium. Further testing is recommended to understand performances with high-potassium wastes such as are found in AP-101 and AW-101 (0.7 M and 0.4 M potassium, normalized to 5 M sodium) Hanford tank wastes.

## CONCLUSIONS

The spherical RF resin physical-property attributes indicate it will likely provide superior hydraulic performance relative to the ground gel formulations in the large-scale plant operation. The spherical RF resin had excellent morphology for ion exchange processing with tight PSD, a uniformly spherical shape, and with low breakage during multi-cycle processing. The shrink-swell characteristic was less severe relative to that of the baseline resin, SuperLig<sup>®</sup>-644.

Based on the results of 3.5 load/elute cycles, the chemical performance of spherical RF was adequate to meet process plant objectives. The cesium load and elution characteristics were reproducible. The resin breakthrough capacities and selectivities in the AZ-102 tank waste matrix were more than adequate to meet plant process requirements. The spherical RF resin eluted as quickly as, and more extensively than, SuperLig<sup>®</sup>-644 and ground-gel RF. Providing the manufacturing process can be scaled up, the spherical RF resin is a viable option for use in the RPP-WTP.

## REFERENCES

1. Boldt, A.L., Borsheim, G.L., and Colton, N.G. (1999) *Standard Inventories of Chemicals and Radionuclides in Hanford Site Tank Wastes*; HNF-SD-WM-TI-740 Rev; 0C, Fluor Hanford: Richland, WA.
2. Harland, C.E. (1994) *Ion Exchange: Theory and Practice*, 2nd Ed.; The Royal Society of Chemistry: Cambridge, UK.

3. Fiskum, S.K., Blanchard, D.L., Jr., and Arm, S.T. (2005) Cesium removal from simulated and actual Hanford tank waste using ion exchange. *Separation Science and Technology*, 40: 51–67.
4. Bibler, J.P., Wallace, R.M., and Bray, L.A. (1990) Testing a new cesium-specific ion exchange resin for decontamination of alkaline high-activity waste. In *Proceedings of the Symposium on Waste Management '90*; Tucson, AZ, 747–751.
5. Bray, L.A., Elovich, R.J., and Carson, K.J. (1990) *Cesium Recovery Using Savannah River Laboratory Resorcinol-Formaldehyde Ion Exchange Resin*; PNL-7273, Pacific Northwest Laboratory: Richland, WA;
6. Bray, L.A., Carlson, C.D., Carson, K.J., DesChane, J.R., Elovich, R.J., and Kurath, D.E. (1996) *Initial Evaluation of Two Organic Resins and Their Ion Exchange Column Performance for the Recovery of Cesium from Hanford Alkaline Wastes*; PNNL-11124, Pacific Northwest National Laboratory: Richland, WA.
7. Hassan, N.M. and Adu-Wusu, K. (2005) Cesium removal from Hanford tank waste solution using resorcinol-formaldehyde resin. *Solvent Extraction and Ion Exchange*, 23: 275–389.
8. Fowley, M.D., Steimke, J.L., Adamson, D.J., Hamm, L.L., Nash, C.A., Restivo, M.L., Shadday, M.A., Steeper, T.J., Aleman, S.E., and King, W.D. (2004) *Ion Exchange Testing with SuperLig® 644 Resin*; WSRC-TR-2003-00514, WSRC, Savannah River Site: Aiken, SC.
9. Hassan, N.M. and Nash, C.A. (2002) *Evaluating Residence Time for SuperLig® 644 Columns with Simulated LAW Envelope B Solution*; WSRC-TR-2002-00163, Savannah River Technology Center: Aiken, SC.
10. Arm, S.T., Blanchard, D.L., and Fiskum, S.K. (2005) Chemical degradation of an ion exchange resin processing salt solutions. *Separation and Purification Technology*, 43: 59–69.
11. Arm, S.T., Blanchard, D.L., Fiskum, S.K., and Weier, D.R. (2003) *Chemical Degradation of SuperLig® 644 Ion Exchange Resin*; PNWD-3315, Battelle—Pacific Northwest Division: Richland, WA.
12. Fiskum, S.K., Blanchard, D.L., Steele, M.J., and Wagner, J.J.. Analysis of spent SuperLig® 644 resin used for cesium removal from hanford tank wastes. *Solvent Extraction and Ion Exchange*, in press.